Topological Flat Bands in Self-Complementary Plasmonic Metasurfaces

Zhixia Xu,[1,2] Xianghong Kong,[3] Jie Chang,[2] Daniel F. Sievenpiper,[4,*,‡] and Tie Jun Cui[1,†,‡]
[1]State Key Laboratory of Millimeter Waves, Southeast University, Nanjing 210096, China
[2]School of Information Science and Technology, Dalian Maritime University, Dalian 116026, China
[3]Department of Electrical and Computer Engineering, National University of Singapore, Singapore 117583, Singapore
[4]Electrical and Computer Engineering Department, University of California San Diego, San Diego, California 92093, USA

(Received 6 June 2022; revised 9 October 2022; accepted 15 November 2022; published 15 December 2022)

Photonics can be confined in real space with dispersion vanishing in the momentum space due to destructive interference. In this Letter, we report the experimental realization of flat bands with nontrivial topology in a self-complementary plasmonic metasurface. The band diagram and compact localized states are measured. In these nontrivial band gaps, we observe the topological edge states by near-field measurements. Furthermore, we propose a digitalized metasurface by loading controllable diodes with C_3 symmetry in every unit cell. By pumping a digital signal into the metasurface, we investigate the interaction between incident waves and the dynamic metasurface. Experimental results indicate that compact localized states in the nontrivial flat band could enhance the wave-matter interactions to convert more incident waves to time-modulated harmonic photonics. Although our experiments are conducted in the microwave regime, extending the related concepts into the optical plasmonic systems is feasible. Our findings pave an avenue toward planar integrated photonic devices with nontrivial flat bands and exotic transmission phenomena.

DOI: 10.1103/PhysRevLett.129.253001

Introduction.—Fermions and bosons can be confined in the real space when any hopping to neighboring cells is hindered by the destructive interface [1], corresponding to a nondispersive flat band in the momentum space, where the energy spectrum $E(\boldsymbol{k})$ is independent of the momentum $\boldsymbol{k}$ [2]. Perfectly flat bands with a zero bandwidth have been widely explored in tight-binding models [3–6], and nearly flat bands with a small bandwidth are also acceptable because perturbation is usually inevitable in practice [7,8]. Various experimental platforms have been proposed, including coupled waveguides [9,10], resonators [11], metasurfaces [12], optical micropillars [13], and twist-bilayer structures [14–16]. Photonic flat bands cause various light transport phenomena and applications [17], such as slow-wave waveguides with reduced dispersion [18,19], superconducting circuits [20,21], and phase-locked coupled lasers [22]. With exploring the nontrivial topology of bands, flat bands with the quantum Hall effect are becoming a fruitful topic in condensed-matter physics, including strong correlation [23], superfluidity, and superconductivity [24,25]. Nontrivial flat bands have been reported in twist-bilayer systems [26–28], kagome lattices [29], triplet excitonic insulator [30], and Chern topological insulators [31–34]. Interactions between these nontrivial flat bands with nonlinear materials [35] or coupled quantum emitters [36] are becoming hot topics.

In this Letter, we propose a self-complementary spoof localized surface plasmonic (LSP) metasurface with nontrivial flat bands. In the topological band gaps, we observed the edge states by near-field measurements. The band diagram was measured by a far-field reflection method to show the flat bands near the Γ point. We also showed that the compact localized states in flat bands could be excited by the incident surface waves from high-symmetric directions, and the waves can pass the structure without distortion. Finally, we implanted controllable diodes into the structure and pumped a digital signal into the metasurface to generate time-modulated compact localized states. The measured spectrum reveals the generation of multiple time-modulated harmonic photonics, whose energy can be enhanced by wave trapping in the flat band. Most observed phenomena in the metasurface can also be found in an ideal two-dimensional optical system by replacing dielectric rods in all-Si valley photonic crystals [37] with plasmonic rods. The optical simulations and the tight-binding models are discussed in the Supplemental Material [38].

Self-complementary spoof LSPs.—According to the Babinet principle [52], the proposed structure consists of self-complementary patches and slots with the same pattern on both sides of the substrate [Fig. 1(a)]. The decorated periodic grooves in the triangular unit cell can enhance the slow-wave performance to generate multiple spoof LSPs [53–56]. The structure combines stacked topological photonic crystals [57] and dual-impedance metasurfaces [58,59]. We find that single-layered spoof LSPs have limited bands below the light cone [60–62]; however, the self-complementary spoof LSPs can generate multiple topological flat bands below the light cone [Fig. 1(b)]. Detailed comparisons between the proposed structure and traditional structures are presented in the Supplemental

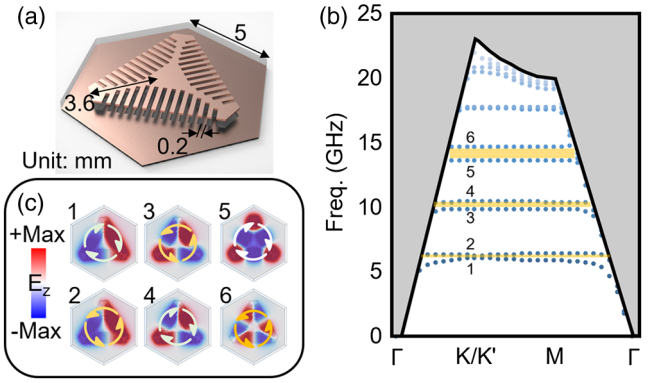

FIG. 1. Eigenmodes of the unit cell. (a) Self-complementary spoof LSPs unit cell. (b) Simulated band diagram. The gray area represents the fast-wave region. (c) Eigenfield distributions and the chirality of the Poynting vectors at the K points.

Material [38]. The C_3-symmetric unit cell belongs to valley photonic topological insulators. Eigenfield distributions are in the same order on both sides of these nontrivial band gaps, but the energy flows show the opposite chirality [Fig. 1(c)].

Topological edge states.—The nontrivial edge states can be supported by two types of interfaces [Fig. 2]. The dispersion in the first band gap is a classical valley transport [37,63], and more edge states exist in the higher-order band gaps [Figs. 2(a) and 2(b)]. Two samples with triangular edge routes are fabricated and measured [Fig. 2(c)]. We establish a near-field scanning system to observe the topological states in the band gaps; see the Supplemental Material for more experimental details [38]. The edge states and bulk modes are directly recorded. The edge states in the first band gap can travel along the triangular route. However, the edge states in the second band gap decay rapidly because of the metallic loss and the leaky wave radiation. The radiation mechanism is similar to that in a Chern waveguide, where fast waves radiate during the propagation process [64]. Reference [65] has studied details about the intrinsic losses in various topological waveguides.

Flat bands.—Different from the flatness defined by the group delay and its variance along transmission direction in waveguides [18], the flatness of the two-dimensional band can be revealed by the fractional bandwidth (FBW) FBW $= 2(\omega_t - \omega_b)/(\omega_t + \omega_b)$, where ω_t and ω_b are the top and bottom frequencies of the objective band within the light cone [66]. In our model, the first band starts from 0 to about 6 GHz, and the whole band is located within the light cone. Therefore, the FBW has the maximum value of 2, representing a dispersive band starting from the Γ point. The FBW of other bands within the light cone is calculated as 0.022, 0.004, 0.009, 0.0015, and 0.0054, respectively. The smaller FBW means a more significant density of states (DOS) [45], in which the waves are better confined in the structure. We analyze an ideal two-dimensional superlattice to reveal the relationship between the flat band, the photonic DOS, and the compact localized states, which are discussed in the Supplemental Material [38].

We further measure the bands by a far-field reflection method [Fig. 3(a)], where the wave vector $\mathbf{k}_{\parallel}$ in the plane of the lattice is represented by the reflection angle θ of the pair of Vivaldi antennas as $\mathbf{k}_{\parallel} = (\omega/c)\cos\theta$. The pair of antennas are rotated from 25° to 85° to obtain the band diagram with varying $\mathbf{k}_{\parallel}$ around the momentum region near the Γ point. The unchanged frequency of the reflection dips reveals the existence of flat bands, representing the maximum excitation of compact localized states in the structure [Fig. 3(b)]. With the strong field enhancement, the energy can be absorbed by the metasurface; hence, the reflection power decreases. Because of the limitation of the performance of antennas, we can conduct measurements from 6 to 12 GHz, where three measured bands match well with simulations.

Undistorted transmission.—In an ideal optical counterpart, we find the undistorted transmission in flat bands by simulations, as shown in the Supplemental Material [38].

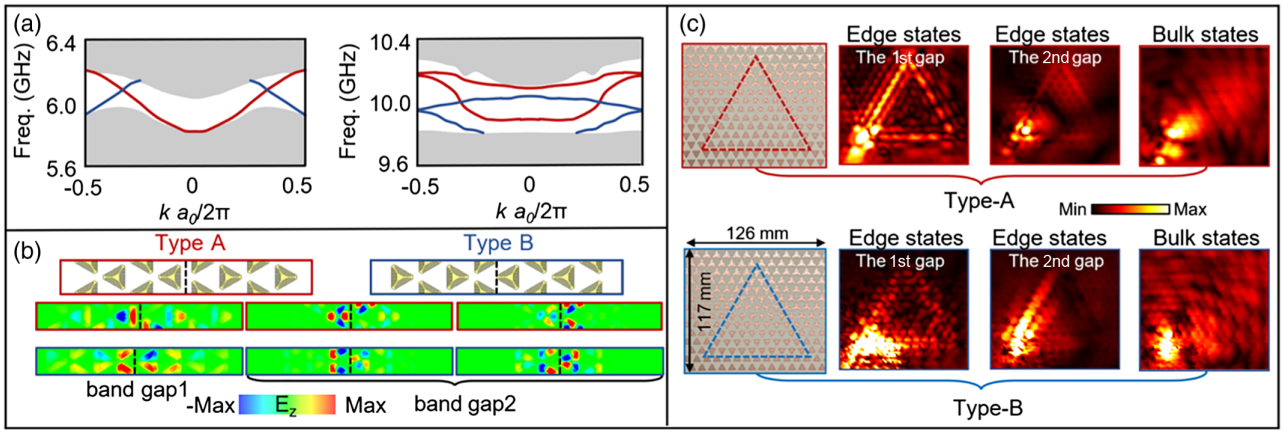

FIG. 2. Topological edge transmission. (a) Edge dispersion in the two band gaps. (b) The corresponding field distributions of edge states. (c) Fabricated samples with triangular interface routes and corresponding near-field experimental results.

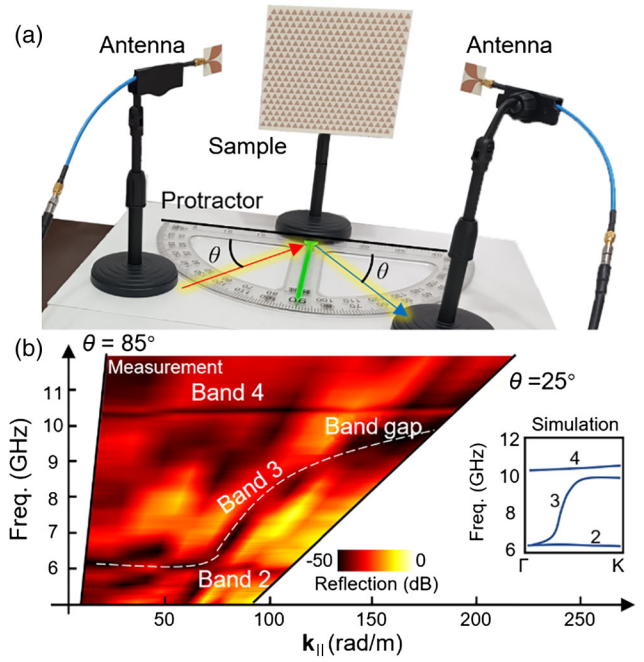

FIG. 3. Measurement of the band diagram. (a) The experimental configuration. (b) The band diagram revealed by the reflection test, where the inset shows the simulated band diagram.

The incident waves from high-symmetric directions can pass the structure ideally without changing the planar wave front. To conduct an analogy experiment, we insert the metasurface in a grid plane, which can support the transmission of surface waves. An array of probes was installed on one side of the mesh grid to generate the surface waves with the planar wave front [Fig. 4(a)]. By simulations and near-field scanning, we observe that the surface waves can excite compact localized states and travel across the metasurface ideally [Fig. 4(b)]. Because of the double-layered structure, the electromagnetic field is well confined in the substrate. Therefore, the electric field on the cross section of the middle of the substrate can reveal the phenomenon better than that on the surface of the structure.

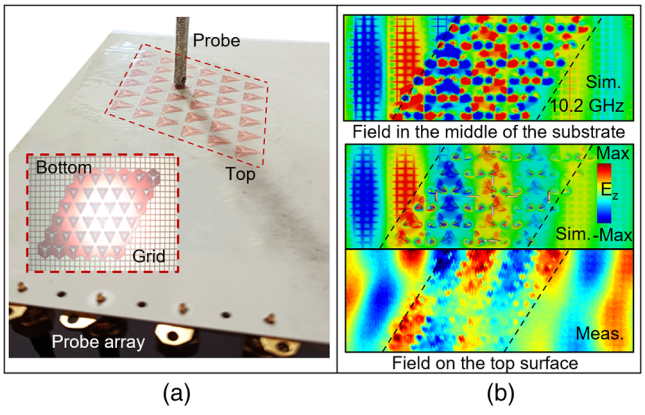

FIG. 4. Surface waves interact with the compact localized states. (a) The sample under test. (b) The simulated and measured near fields around 10.2 GHz.

Time-modulated harmonic photonics.—The flat bands can bring strong wave trapping due to the related compact localized states; therefore, the enhanced interaction with materials is a promising research direction [67]. Here, we report the enhanced wave-matter interactions to generate time-modulated harmonic photonics. We implant three diodes (SMP1320) in every unit cell with the C_3 symmetry. Every unit cell is connected to the digital pins of a microcontroller (Arduino Mega 2560). By pumping a square-wave signal, we dynamically shift the open-short state of the diodes [Fig. 5(a)]. When the diodes are biased with 5 V voltage, the unit cell is in the short state where the up and bottom patches are connected, and the whole structure behaves as one piece of a metallic surface. However, without the bias voltage, the diodes are in the open state, and the unit cell retains the same characteristics as before. The performance of diodes limits the maximum working frequency. With the frequency of incident waves increasing above 12 GHz, the losses increase dramatically. Therefore, we conduct experiments from 5 to 12 GHz and observe that the nontrivial flat band can enhance the generation of time-modulated harmonic photonics. The metasurface is pumped by a digital square-wave signal with the frequency $f_M = 1.6$ MHz. We connect an antenna to the signal generator to emit continuous waves of frequency f_{in} and place a probe on the surface of the structure to detect the trapped waves in the metasurface [Fig. 5(b)]. The multiple time-modulated harmonic photonics appear at discrete frequencies $f_{\text{in}} \pm nf_M$ $(n = 0, \pm 1, \pm 2, \ldots)$. We sweep the frequency of incident waves and record the corresponding trapping spectrum [Fig. 5(c)]. The harmonic converting efficiency is calculated as $E = \sum P_n / P_{\text{in}}$, where P_n is the power of the nth-order harmonic and P_{in} is the total incident power. Around 9.5 GHz, the electromagnetic waves are dramatically trapped to enhance the time-modulated harmonic photonics. The converting efficiency achieves about 90%, and in the corresponding spectrum, the peak at f_{in} is much lower than the time-modulated harmonic photonics [Fig. 5(d)]. These results confirm the applications of the self-complementary topological metasurface in the field of wave-matter enhancements.

Optical and tight-binding models.—In order to show the generality of our findings, multiple nontrivial flat bands are explored in an optical photonic crystal, which consists of plasmonic rods arranged in the honeycomb lattice, and similar phenomena could be found in the optical region, as shown in the Supplemental Material [38]. Furthermore, a tight-binding model whose band diagram and topological properties have an excellent match to those in the plasmonic structure is also discussed in the Supplemental Material [38]. Analytical tools, such as the Berry phase, Wannier function, and Wilson loop, are applicable to both fermionic and bosonic systems [49]. The concept of

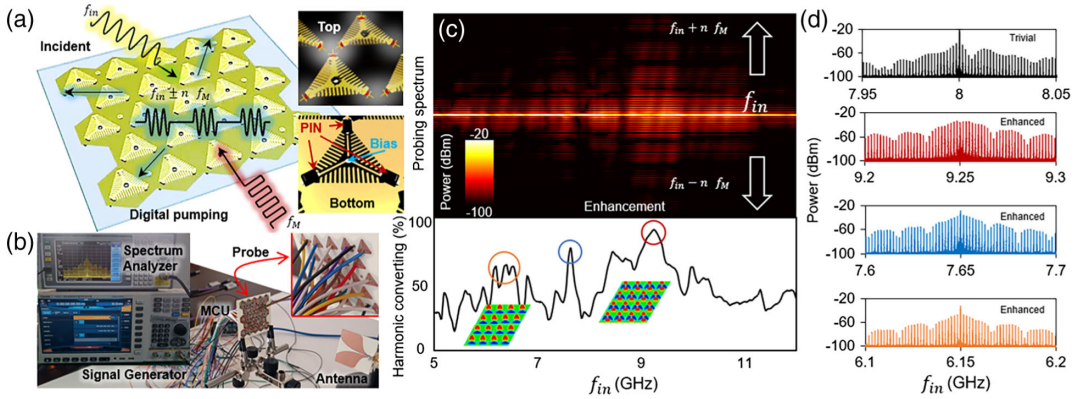

FIG. 5. Time-modulated harmonic photonics. (a) Digitalized topological metasurface by loading diodes with C_3 symmetry. (b) Experimental environment. (c) Spectral map with varying frequency of incident waves and calculated harmonic converting efficiency, in which the time-modulated harmonics are enhanced due to the compact localized states. (d) Different spectral distributions without the enhancement (black) and with the enhancement caused by the quadrupole spoof LSP modes (red), the resonance shift caused by PIN diodes (blue), and the dipole spoof LSP modes (orange).

electron charges can be associated with the Poynting vector and energy density of electromagnetic fields [46].

Conclusion.—We propose a self-complementary spoof plasmonic metasurface to support nontrivial flat bands. In this platform, we explore various transmission and trapping phenomena based on a series of designed experiments, including the multiband topological edge states, the compact localized states, and the undistorted transmission in the flat bands. On top of that, we digitalize the platform by implanting diodes into the unit cell. The interactions between the compact localized states in the flat band and the pumping digital signals are enhanced to generate time-modulated harmonic photonics. This Letter paves the way for highly integrated photonic devices, where the flat bands and nontrivial topology can induce various types of transports and wave-matter interactions.

The near-field and far-field experiments are conducted using Rohde & Schwarz ZNA43. Wide-band signal scans and spectrum records are based on the Ceyear 1465D-V signal generator and the Ceyear 4037 spectrum analyzer. The authors would like to thank X. Yin and H. Zhao for helping improve the quality of the experimental setups, H. Wu and Z. Xiong for valuable discussions about the time-modulation technology, and J. Tong and Q. Zhang for providing Vivaldi antennas for far-field measurements. This work was supported by the Basic Scientific Center of Information Metamaterial of the National Natural Science Foundation of China (Grant No. 62288101), the National Key Research and Development Program of China (Grant No. 2017YFA0700201-3), the State Key Laboratory of Millimeter Waves (Grant No. K202202), and Fundamental Research Funds for the Central Universities (Grant No. 3132022240).

*dsievenpiper@eng.ucsd.edu
†tjcui@seu.edu.cn
‡To whom correspondence should be addressed.

[1] N. Regnault *et al.*, Nature (London) **603**, 824 (2022).
[2] D. Leykam, A. Andreanov, and S. Flach, Adv. Phys. **3**, 1473052 (2018).
[3] W. Maimaiti, A. Andreanov, and S. Flach, Phys. Rev. B **103**, 165116 (2021).
[4] L. Morales-Inostroza and R. A. Vicencio, Phys. Rev. A **94**, 043831 (2016).
[5] M. Röntgen, M. Pyzh, C. V. Morfonios, N. E. Palaiodimopoulos, F. K. Diakonos, and P. Schmelcher, Phys. Rev. Lett. **126**, 180601 (2021).
[6] C. V. Morfonios, M. Röntgen, M. Pyzh, and P. Schmelcher, Phys. Rev. B **104**, 035105 (2021).
[7] Y. Huang, P. Hosur, and H. K. Pal, Phys. Rev. B **102**, 155429 (2020).
[8] K. Sun, Z. Gu, H. Katsura, and S. Das Sarma, Phys. Rev. Lett. **106**, 236803 (2011).
[9] S. Mukherjee, A. Spracklen, D. Choudhury, N. Goldman, P. Öhberg, E. Andersson, and R. R. Thomson, Phys. Rev. Lett. **114**, 245504 (2015).
[10] S. Xia *et al.*, Phys. Rev. Lett. **121**, 263902 (2018).
[11] T. Jacqmin, I. Carusotto, I. Sagnes, M. Abbarchi, D. D. Solnyshkov, G. Malpuech, E. Galopin, A. Lemaître, J. Bloch, and A. Amo, Phys. Rev. Lett. **112**, 116402 (2014).
[12] Y. Nakata, T. Okada, T. Nakanishi, and M. Kitano, Phys. Rev. B **85**, 205128 (2012).
[13] F. Baboux *et al.*, Phys. Rev. Lett. **116**, 066402 (2016).
[14] K. Dong, T. Zhang, J. Li, Q. Wang, F. Yang, Y. Rho, D. Wang, C. P. Grigoropoulos, J. Wu, and J. Yao, Phys. Rev. Lett. **126**, 223601 (2021).
[15] S. Lisi *et al.*, Nat. Phys. **17**, 189 (2021).
[16] H. Tang, F. Du, S. Carr, C. DeVault, O. Mello, and E. Mazur, Light Sci. Appl. **10**, 157 (2021).
[17] D. Leykam and S. Flach, APL Photonics **3**, 070901 (2018).

[18] J. Li, T. P. White, L. O'Faolain, A. Gomez-Iglesias, and T. F. Krauss, Opt. Express **16**, 6227 (2008).
[19] H. Gersen, T. J. Karle, R. J. P. Engelen, W. Bogaerts, J. P. Korterik, N. F. van Hulst, T. F. Krauss, and L. Kuipers, Phys. Rev. Lett. **94**, 073903 (2005).
[20] X. Gu, A. F. Kockum, A. Miranowicz, Y. Liu, and F. Nori, Phys. Rep. **718–719**, 1 (2017).
[21] L. Chirolli and J. E. Moore, Phys. Rev. Lett. **126**, 187701 (2021).
[22] M. Nixon, E. Ronen, A. A. Friesem, and N. Davidson, Phys. Rev. Lett. **110**, 184102 (2013).
[23] M. Kang *et al.*, Nat. Commun. **11**, 4004 (2020).
[24] F. Xie, Z. Song, B. Lian, and B. A. Bernevig, Phys. Rev. Lett. **124**, 167002 (2020).
[25] D. Călugăru, A. Chew, L. Elcoro, Y. Xu, N. Regnault, Z.-D. Song, and B. A. Bernevig, Nat. Phys. **18**, 185 (2022).
[26] D.-S. Ma, Y. Xu, C. S. Chiu, N. Regnault, A. A. Houck, Z. Song, and B. A. Bernevig, Phys. Rev. Lett. **125**, 266403 (2020).
[27] S. Wu, Z. Zhang, K. Watanabe, T. Taniguchi, and E. Y. Andrei, Nat. Mater. **20**, 488 (2021).
[28] X. Liu, C.-L. Chiu, J. Y. Lee, G. Farahi, K. Watanabe, T. Taniguchi, A. Vishwanath, and A. Yazdani, Nat. Commun. **12**, 2732 (2021).
[29] H. Xue, Y. Yang, F. Gao, Y. Chong, and B. Zhang, Nat. Mater. **18**, 108 (2019).
[30] G. Sethi, Y. Zhou, L. Zhu, L. Yang, and F. Liu, Phys. Rev. Lett. **126**, 196403 (2021).
[31] Y. Zhou, G. Sethi, C. Zhang, X. Ni, and F. Liu, Phys. Rev. B **102**, 125115 (2020).
[32] E. J. Bergholtz and Z. Liu, Int. J. Mod. Phys. B **27**, 1330017 (2013).
[33] Z. Liu, E. J. Bergholtz, H. Fan, and A. M. Läuchli, Phys. Rev. Lett. **109**, 186805 (2012).
[34] S. Yang, Z.-C. Gu, K. Sun, and S. Das Sarma, Phys. Rev. B **86**, 241112(R) (2012).
[35] C. Danieli, A. Andreanov, T. Mithun, and S. Flach, Phys. Rev. B **104**, 085131 (2021).
[36] J. Perczel, J. Borregaard, D. E. Chang, S. F. Yelin, and M. D. Lukin, Phys. Rev. Lett. **124**, 083603 (2020).
[37] T. Ma and G. Shvets, New J. Phys. **18**, 025012 (2016).
[38] See Supplemental Material at http://link.aps.org/supplemental/10.1103/PhysRevLett.129.253001 for additional information on the microwave experiments, the optical system, and the tight-binding model, which includes Refs. [5,6,39–51].
[39] Z. Xu, J. Chang, J. Tong, D. F. Sievenpiper, and T. J. Cui, Adv. Opt. Photonics **4**, 046004 (2022).
[40] D. J. Bisharat and D. F. Sievenpiper, Phys. Rev. Lett. **119**, 106802 (2017).
[41] Z. Xu, X. Yin, and D. F. Sievenpiper, Phys. Rev. Appl. **11**, 044071 (2019).
[42] D. Vanderbilt, *Berry Phases in Electronic Structure Theory: Electric Polarization, Orbital Magnetization and Topological Insulators*, 1st ed. (Cambridge University Press, Cambridge, England, 2018).
[43] F. J. García de Abajo and M. Kociak, Phys. Rev. Lett. **100**, 106804 (2008).
[44] R. C. McPhedran, L. C. Botten, J. McOrist, A. A. Asatryan, C. M. de Sterke, and N. A. Nicorovici, Phys. Rev. E **69**, 016609 (2004).
[45] W. Maimaiti, B. Dietz, and A. Andreanov, Phys. Rev. B **102**, 214301 (2020).
[46] M. B. de Paz, M. A. J. Herrera, P. A. Huidobro, H. Alaeian, M. G. Vergniory, B. Bradlyn, G. Giedke, A. García-Etxarri, and D. Bercioux, J. Phys. Condens. Matter **34**, 314002 (2022).
[47] Z. Xu, X. Kong, R. J. Davis, D. Bisharat, Y. Zhou, X. Yin, and D. F. Sievenpiper, Phys. Rev. Res. **2**, 013209 (2020).
[48] W. A. Benalcazar, T. Li, and T. L. Hughes, Phys. Rev. B **99**, 245151 (2019).
[49] Y. Liu, S. Leung, F.-F. Li, Z.-K. Lin, X. Tao, Y. Poo, and J.-H. Jiang, Nature (London) **589**, 381 (2021).
[50] C. W. Peterson, T. Li, W. Jiang, T. L. Hughes, and G. Bahl, Nature (London) **589**, 376 (2021).
[51] X. Huang, Y. Lai, Z. H. Hang, H. Zheng, and C. T. Chan, Nat. Mater. **10**, 582 (2011).
[52] F. Falcone, T. Lopetegi, M. A. G. Laso, J. D. Baena, J. Bonache, M. Beruete, R. Marqués, F. Martín, and M. Sorolla, Phys. Rev. Lett. **93**, 197401 (2004).
[53] F. J. Garcia-Vidal, A. I. Fernández-Domínguez, L. Martin-Moreno, H. C. Zhang, W. Tang, R. Peng, and T. J. Cui, Rev. Mod. Phys. **94**, 025004 (2022).
[54] X. Shen and T. J. Cui, Laser Photonics Rev. **8**, 137 (2014).
[55] Z. Gao, L. Wu, F. Gao, Y. Luo, and B. Zhang, Adv. Mater. **30**, 1706683 (2018).
[56] Z. Xu, Y. Wang, J. Chang, and T. J. Cui, Phys. Rev. Appl. **18**, 024035 (2022).
[57] Y. Zeng *et al.*, Nature (London) **578**, 246 (2020).
[58] O. Yermakov, V. Lenets, A. Sayanskiy, J. Baena, E. Martini, S. Glybovski, and S. Maci, Phys. Rev. X **11**, 031038 (2021).
[59] Z. Xu, J. Chang, S. Fang, Q. Zhang, R. J. Davis, D. Sievenpiper, and T. J. Cui, ACS Photonics **8**, 2285 (2021).
[60] J. W. You, Q. Ma, Z. Lan, Q. Xiao, N. C. Panoiu, and T. J. Cui, Nat. Commun. **12**, 5468 (2021).
[61] X. Wu, Y. Meng, J. Tian, Y. Huang, H. Xiang, D. Han, and W. Wen, Nat. Commun. **8**, 1304 (2017).
[62] F. Gao *et al.*, Nat. Commun. **7**, 11619 (2016).
[63] Y. Yang, Y. Yamagami, X. Yu, P. Pitchappa, J. Webber, B. Zhang, M. Fujita, T. Nagatsuma, and R. Singh, Nat. Photonics **14**, 446 (2020).
[64] Z. Xu, M. Wang, S. Fang, H. Liu, Z. Wang, and D. F. Sievenpiper, IEEE Trans. Antennas Propag. **70**, 2358 (2022).
[65] E. Sauer, J. P. Vasco, and S. Hughes, Phys. Rev. Res. **2**, 043109 (2020).
[66] H. Takeda, T. Takashima, and K. Yoshino, J. Phys. Condens. Matter **16**, 6317 (2004).
[67] V. Goblot *et al.*, Phys. Rev. Lett. **123**, 113901 (2019).